Dalton Transactions

Accepted Manuscript

This is an *Accepted Manuscript*, which has been through the Royal Society of Chemistry peer review process and has been accepted for publication.

Accepted Manuscripts are published online shortly after acceptance, before technical editing, formatting and proof reading. Using this free service, authors can make their results available to the community, in citable form, before we publish the edited article. We will replace this *Accepted Manuscript* with the edited and formatted *Advance Article* as soon as it is available.

You can find more information about *Accepted Manuscripts* in the Information for Authors.

Please note that technical editing may introduce minor changes to the text and/or graphics, which may alter content. The journal's standard Terms & Conditions and the Ethical guidelines still apply. In no event shall the Royal Society of Chemistry be held responsible for any errors or omissions in this *Accepted Manuscript* or any consequences arising from the use of any information it contains.

ROYAL SOCIETY OF CHEMISTRY

www.rsc.org/dalton

Dalton Transaction: Revised

May 2015

Improved Selectivity for Pb(II) by Sulfur, Selenium and Tellurium Analogues of 1,8-Anthraquinone-18-Crown-5: Synthesis, Spectroscopy, X-ray Crystallography and Computational Studies

Kadarkaraisamy Mariappan*, Madhubabu Alaparthi, Mariah Hoffman, Myriam Alcantar Rama, Vinothini Balasubramanian, Danielle M John, and Andrew G Sykes

Contribution from the Department of Chemistry
University of South Dakota, Vermillion, SD 57069

*To whom correspondence should be addressed: mkadarka@usd.edu

Dalton Transactions Accepted Manuscript

Abstract:

We report here a series of heteroatom-substituted macrocycles containing an anthraquinone moiety as a fluorescent signaling unit and a cyclic polyheteroether chain as the receptor. Sulfur, selenium, and tellurium derivatives of 1,8-anthraquinone-18-crown-5 (**1**) were synthesized by reacting sodium sulfide (Na_2S), sodium selenide (Na_2Se) and sodium telluride (Na_2Te) with 1,8-bis(2-bromoethylethyleneoxy)anthracene-9,10-dione in a 1:1 ratio. The optical properties of the new compounds are examined and the sulfur and selenium analogues produce an intense green emission enhancement upon association with Pb(II) in acetonitrile. Selectivity for Pb(II) is markedly improved as compared to the oxygen analogue **1** which was also competitive for Ca(II) ion. UV-Visible and luminescence titrations reveal that **2** and **3** form 1:1 complexes with Pb(II), confirmed by single-crystal X-ray studies where Pb(II) is complexed within the macrocycle through coordinate covalent bonds to neighboring carbonyl, ether and heteroether donor atoms. Cyclic voltammetry of **2**-**8** showed classical, irreversible oxidation potentials for sulfur, selenium and tellurium heteroethers in addition to two one-electron reductions for the anthraquinone carbonyl groups. DFT calculations were also conducted on **1**, **2**, **3**, **6, 6**+Pb(II) and **6**+Mg(II) to determine the trend in energies of the HOMO and the LUMO levels along the series.

Keywords: Anthraquinone; Thioether; Selenoether; Telluroether; Fluorescent Sensor, Pb(II) selectivity

Dalton Transactions Accepted Manuscript

Introduction

Many reports have been devoted to the design of new metal ion sensors for various potential applications such as clinical toxicology, eco-friendly bioorganic chemistry, bioremediation and waste administration.[1] The exposure of heavy meal ions to humans, animals and ecological systems cause's neurodegenerative diseases such as Alzheimer's (AD), Prion (PrPD) diseases, Parkinson's disease (PD), Huntington disease (HD), Amyotrophic Lateral Sclerosis (ALS), and many more.[2] Lead ranks as the second most toxic heavy metal ion next to mercury, and is often encountered due to its wide distribution in old batteries, paints and gasoline.[3] Many quantitative methods, such as atomic absorption spectroscopy (AAS), inductively coupled plasma atomic emission spectroscopy (ICP-AES), X-ray fluorescence spectroscopy (R-FS)[4] and potentiometric methods[5], are available to detect heavy metal ions; however more compatible and less expensive molecular sensor devices have replaced these techniques in recent years.[6] Molecular sensors based on luminescent and colorimetric detection are more attractive due to their simplicity and low detection limits even at the nanomolar level. Luminescent probes of the OFF-ON type are more advantageous tools because of their sensitivity to the availability of the analyte, especially important at low concentration of analyte. The mechanisms described in the literature for the luminescence changes when detecting metal ions, anions or small molecules are mainly based on internal charge transfer (ICT)[7], twisted internal charge transfer (TICT)[8] photoinduced electron transfer (PET)[9], fluorescence resonance energy transfer (FRET & TBET)[10], photoinduced charge transfer (PCT)[11], metal to ligand charge transfer (MLCT)[12], chelation enhanced fluorescence (CHEF)[13] excited state intramolecular proton transfer (ESIPT)[14], excimer & exciplex[15] complex formation and the inversion of excited states (n-π^* and π-π^*).[16]

Dalton Transactions Accepted Manuscript

Substantial effort has been paid to the synthesis of anthraquinone compounds in recent years due to their application as colorants[17], as models for photosynthesis[18] and as DNA intercalators.[19] 9,10-Anthraquinone (AQ) compounds substituted at various positions have served as ligands for a variety of metal ions as recently described in a review article.[20] Anthraquinone derivatives have been exploited as an efficient colorimetric chemosensors for the detection of metal ions and anions due to their very high absorption coefficient.[21] Apart from their optical properties, anthraquinone derivatives are also very popular for electroanalytical chemistry because of the quinone moiety, as they show two successive, reversible, one electron reductions[22] to form AQ^{1-} followed by AQ^{2-}. In our own work, we have reported several fluorescent host molecules that contain the anthraquinone moiety as a sensing unit connected with a polyether receptor for the detection of toxic heavy metal ions. For example, 1,8-anthraquinone-18-crown-5 (**1**) is composed of AQ and a polyether chain substituted at the 1,8-positions, and it has been reported as a redox switch for alkali metal ions[22], a luminescent probe for oxo-acid[23], a luminescent sensor for the detection of Pb(II)[24], and, in its reduced form, is the precursor for making molecular switches.[25] Furthermore, the replacement of the hard donor oxygen atoms by the soft donor sulfur in the polyether chain of **1** dramatically changes the selectivity of this class of sensor.[26] Apart from identity of the donor atoms, the emission intensity of 1,8-oxygen substituted AQ derivative with analytes depends not only on the identity and position of substitution, but also on the ring size of the macrocycle, and the length of the side chains if the receptor is an open bipodand.[27-28] Additional heteroatom substitutions at the anthraquinone and the coordination chemistry of metal ions with anthraquinone-containing macrocycles have also been reported.[29-34] The field of synthetic organoselenium / tellurium chemistry is as active as anthraquinone chemistry due to probable applications in medicinal

Dalton Transactions Accepted Manuscript

chemistry and in materials chemistry. In particular, selenium heterocyclic compounds are well known for their biological and pharmacological applications as anti-oxidants, anti-fungal, anti-inflammatory and anti-bacterial agents.[35-37] Sulfur, selenium and tellurium at lower oxidation states are softer donors than their oxygen counterpart and their ligand chemistry has been extensively reviewed[38]. Recent reports reveal that sulfur[39], selenium[40] and tellurium[41] compounds have emerged as potential sensors for the detection of metal ions and other active species by luminescence spectroscopy. The transport properties of Ag(I) and Pb(II) by selenium crown ether based compounds has also been reported.[42] Lead (II) complexes of oxygen, sulfur and selenium donors have been previously reviewed.[43]

In this paper, we report the synthesis of new luminescent sensors, thio-18-crown-5 (**2**), seleno-18-crown-5 (**3**) and telluro-18-crown-5 (**6**) which contain softer Lewis donors and improve the selectivity of these sensors for Pb(II) over the previously reported oxygen analogue.[24] The presence of hard and soft donors in the polyether chain was used to tune the selectivity and the optical properties of the luminescent sensors. X-ray crystallography of sulfur and selenium analogues and their Pb(II) complexes are included and the experimental findings are supported by theoretical computations on these new heteroatom macrocycles and their Pb(II) adducts.

Dalton Transactions Accepted Manuscript

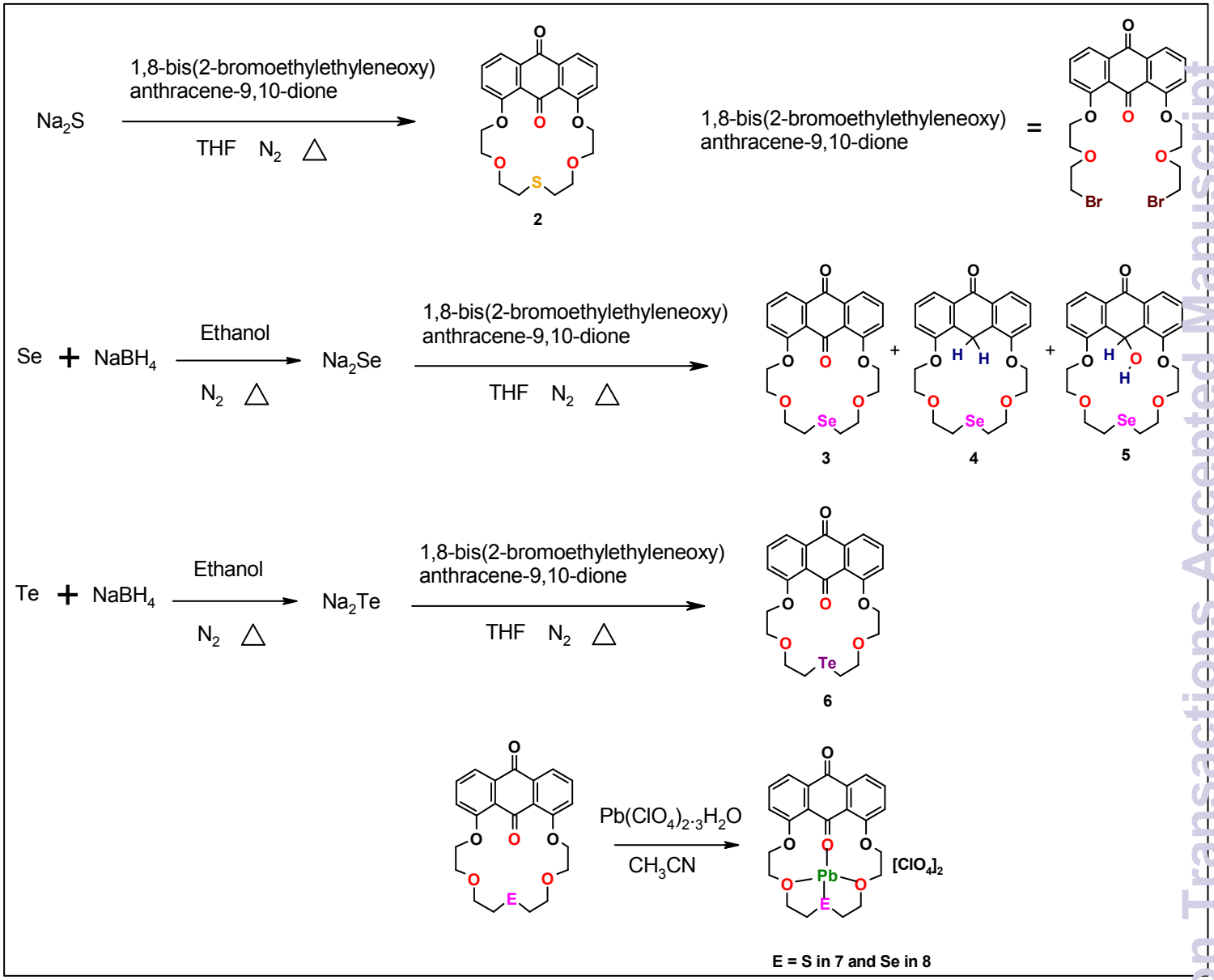

Scheme 1: Elemental selenium and tellurium were reduced by $NaBH_4$ in alcohol to obtain Na_2Se or Na_2Te under N_2. Compound **4** and **5** were isolated during **3**'s synthesis, and they can also be made by mixing **3** with $NaBH_4$.

Results:

Dalton Transactions Accepted Manuscript

Synthesis: Three new cyclic anthraquinone-based polyether derivatives, **2**, **3** and **6**, have been synthesized by a double S_N2 reaction between 1,8-bis(2-bromoethoxy)anthracene-9,10-dione with the appropriate sodium chalcogenide (Scheme 1). Compound **2** is obtained in 65% yield; whereas **3** and **6** are obtained only in 25% and 10% respectively. Na_2E (E = Se and Te) is produced by the reaction of Se/Te with $NaBH_4$, and the in situ synthesis of **3** also produces compounds **4** and **5** since the reducing agent is present in an excess (Scheme 1). The reaction of $Pb(ClO_4)_2.3H_2O$ with **2** and **3** in a 1:1 ratio, using acetonitrile as a solvent, affords the yellow/orange colored complexes $[Pb(\mathbf{2})][ClO_4]_2$ (**7**) and $[Pb(\mathbf{3})][ClO_4]_2$ (**8**) in more than 50% yield. A schematic representation of compound **2-8** is given in Scheme 1. Compounds **2-8** are stable under ambient conditions and are very soluble in CH_2Cl_2, $CHCl_3$, CH_3CN and a CH_3CN:CH_3OH mixture.

NMR Spectroscopy: The ^1H NMR spectra of **2-6** were recorded using $CDCl_3$ solutions at room temperature. All five new anthraquinone based cyclic crown ethers, including the reduced compounds of **3,** exhibit a doublet, a triplet and a doublet pattern in the aromatic region due to 1,8-disubstituted anthraquinone as per literature reports. [22-28] A triplet at ~ 2.9 ppm in **2-6** is due to the CH_2- connected to the chalcogenides. Singlet resonances at 4.12 and 6.27 ppm are from the anthrone and anthronol protons respectively in **4** and **5** which support the reduction of one of the carbonyl groups in each compound. In the ^{13}C spectra of **2-6**, the CH_2-E (E = S, Se and Te) signal appears at 31.8, 23.3, 23.8, 23.1 and 12.1 respectively. The appearance of a signal at 22.7 ppm in **4** and at 57.2 ppm in **5** is due to anthrone and anthronol carbon, respectively. The CH_2-S and the CH_2-Se signal in compounds **2** and **3** underwent a downfield shift of 0.3 ppm (^1H NMR) and ~3.0 ppm (^{13}C NMR) in **7** and **8** which supports the coordination of the sulfur and selenium heteroatoms by the Pb(II) ion. A copy of proton and ^{13}C NMR spectra of compounds **2-8** are

Dalton Transactions Accepted Manuscript

shown in SI Fig.1-14. Elemental analyses and ESI mass spectrometry by direct injection method (SI Fig.15) of **6** supports the proposed structure of **6** in Scheme 1.

Dalton Transactions Accepted Manuscript

Table 1: Crystallographic data for compounds **2**, **3, 4, 5, 7** and **8**.

Compounds	**2**	**3**	**4**	**5**	**7**	**8**
Empirical formula	$C_{22}H_{22}O_6S$	$C_{22}H_{22}O_6Se$	$C_{22}H_{24}O_5Se$	$C_{22}H_{24}O_6Se$	$C_{22}H_{22}Cl_2O_{14}PbS$	$C_{22}H_{22}Cl_2O_{14}PbSe$
Formula weight	414.46	461.36	447.37	463.37	820.54	867.44
Wavelength	MoK_α 0.71073	MoK_α 0.71073	MoK_α 0.71073	MoK_α 0.71073	MoK_α 0.71073	MoK_α 0.71073
System	SMART APEXII	SMART APEXII	SMART APEXII	SMART APEXII	SMART APEXII	SMART APEXII
Temperature, K	100(2)	100(2)	100(2)	100(2)	100(2)	100(2)
Crystal system	Monoclinic	Monoclinic	Monoclinic	Monoclinic	Triclinic	Triclinic
Space group	P21/n	P21/c	P21/n	P21/c	P-1	P-1
a, Å	14.3298(15)	7.4979(8)	14.6414(8)	12.3365(8)	8.0605(6)	8.0759(6)
b, Å	8.1440(8)	16.0574(17)	8.0187(4)	11.5354(8)	12.1558(10)	12.2739(9)
c, Å	16.8072(17)	16.3759(17)	16.9048(9)	14.4592(9)	13.1591(10)	13.1224(9)
α, °	90.00	90.00	90.00	90.00	80.0900(10)	80.0990(10)
β, °	104.2090(10)	100.5730(10)	104.1850(10)	99.2400(10)	82.6810(10)	82.5590(10)
γ, °	90.00	90.00	90.00	90.00	85.4590(10)	85.9020(10)
Volume, $Å^3$	1901.4(3)	1938.1(4)	1924.19(18)	2030.9(2)	1257.60(17)	1268.95(16)
Z	4	4	4	4	2	2
Density (calc)$g.cm^{-3}$	1.448	1.581	1.544	1.515	2.16	2.270
Absorb. Coef. Mm^{-1}	0.209	1.975	1.983	1.885	7.079	8.421
F(000)	872	944	920	952	796	832
θ range	2.50-25.30	2.53-25.30	2.49-25.38	2.43-25.39	2.51-25.46	2.50-25.44
Index ranges	±17, ±9, ±20	±9, ±19, ±19	±17, ±9, ±20	±14, ±13, ±17	±9, ±14, ±15	±9, ±14, ±15
Reflections collected	18441	18948	18815	19801	12675	13047
Independent reflections	3473	3535	3107	3339	4662	4691
Observed reflections	2517	2578	3538	3738	4575	4439
Max/Min trans.	0.901-0.936	0.4383-0.6934	0.3374-0.5876	0.3975-0.4524	0.332-0.538	0.494258 -0.745758
Data / restr. / param.	3473 / 180 / 319	3535/ 67 / 274	3107 / 0 / 253	3339 / 0 / 262	4662 / 0 / 361	4691/ 0 / 360
Goodness-of-fit	1.031	1.061	1.056	1.045	1.065	1.071
Final R indices[$I>2\sigma(I)$]	0.0423	0.0395	0.0237	0.0242	0.0158	0.0242
R indices (all data)	0.0654	0.0671	0.0297	0.0293	0.0162	0.0127
CCDC Number	980449	980451	980452	980453	980450	980454

Dalton Transactions Accepted Manuscript

Table 2: Selected bond lengths (Å) and bond angles (°) of **2**, **3, 4, 5, 7** and **8.**

	2	**3**	**4**	**5**	**7**	**8**
C18-E1	1.806(5)	1.944(4)	1.9567(19)	1.961(2)	1.826(3)	1.961(4)
C19-E1	1.809(5)	1.946(4)	1.9511(19)	1.9585(19)	1.820(3)	1.966(4)
C7-O5	1.220(2)	1.221(5)	1.224 (2)	1.226(2)	1.219(3)	1.209(5)
C8-O6 (C=O)	1.216(2)	1.233(9)	-	1.445(2)	1.229(3)	1.236(5)
Pb1-E1	-	-	-	-	2.8949(7)	2.9904(5)
Pb1-O6 (C=O)	-	-	-	-	2.6003(17)	2.604(3)
Pb1-O7	-	-	-	-	2.6284(19)	2.625(3)
Pb1-O3 (C-O)	-	-	-	-	2.6334(17)	2.642(3)
C18-E1-C19	104.5(3)	100.63(16)	99.30(8)	98.31(8)	103.46(12)	101.5(3)
E1-Pb1-O6(C=O)	-	-	-	-	161.00(4)	160.92(6)
E1-Pb1-O3	-	-	-	-	68.21(4)	70.55(6)

E = S in **2** and **7**; E = Se in **3**, **4** and **5**

Dalton Transactions Accepted Manuscript

X-ray crystallography: The molecular structures of all compounds were determined by single-crystal X-ray diffraction studies, except for compound **6**. The crystallographic data are given in Table 1, and selected bond distances and angles are listed in Table 2. The slow evaporation of a solution of methylene chloride and **2** or **3** gave X-ray quality crystals. The thermal ellipsoid diagrams of **2** and **3** are shown in Fig. 1. CH_2-S bond lengths C18-S1=1.806 Å; C19-S1=1.809 Å, and CH_2- Se bond lengths C18-Se1= 1.944 Å; C19-Se1=1.946 Å are in good agreement with the literature[34b,34c], and the geometry around sulfur and selenium is bent with bond angles C18-S1-C19 and C18-Se1-C19 of 104.5° and 100.63° respectively.

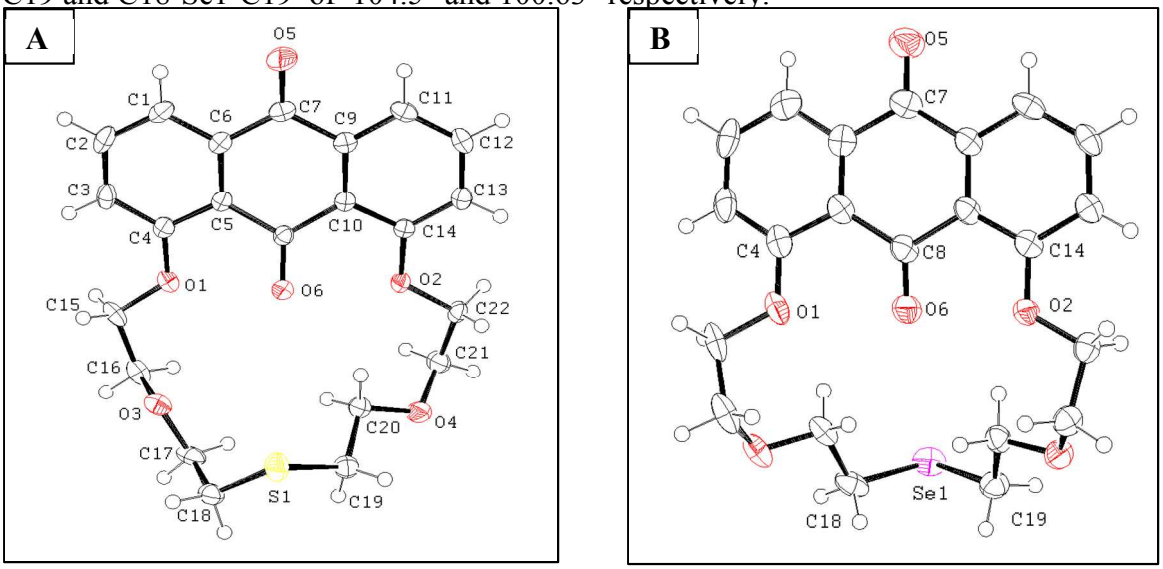

Fig. 1: Thermal ellipsoid diagrams of **2** (A) and **3** (B). For bond angles and bond lengths comparison, identical labeling done on non-hydrogen atoms in both structures except for the chalcogenide. Fragments from disorder is omitted for clarity.

The geometry around C7 and C8 is trigonal planar, and the carbonyl bond lengths, C7-O5 (1.220 Å) and C8-O6 (1.216 Å) in **2** and C7-O5 (1.221 Å); C8-O6 (1.233 Å) in **3,** are typical C=O double bonds. [23 and 24] Thermal ellipsoid diagrams of the reduced macrocycles **4** and **5** are shown in Fig. 2 where CH_2-Se bond lengths in **4** are C18-Se1=1.957Å and C19-Se1=1.951 Å; and in **5** are C18-Se1=1.961 Å and C19-Se1=1.958 Å, in good agreement with earlier reports.[34c] The bond angles around selenium (C18-Se1-C19) are 99.30° and 98.31° which is a slightly distorted

Dalton Transactions Accepted Manuscript

bent geometry, typical of heavier chacogenides. In structures **4** and **5,** the inner carbonyl is missing, and the C8-O6 bond length is 1.445 Å in **5**, which confirms it is a single bond, not a C=O double bond. [25, 44] The carbonyl group bond lengths, C7-O5, in **4** and **5** are 1.224 Å and 1.226 Å, respectively. The geometries around C8 in **4** and **5** are tetrahedral.

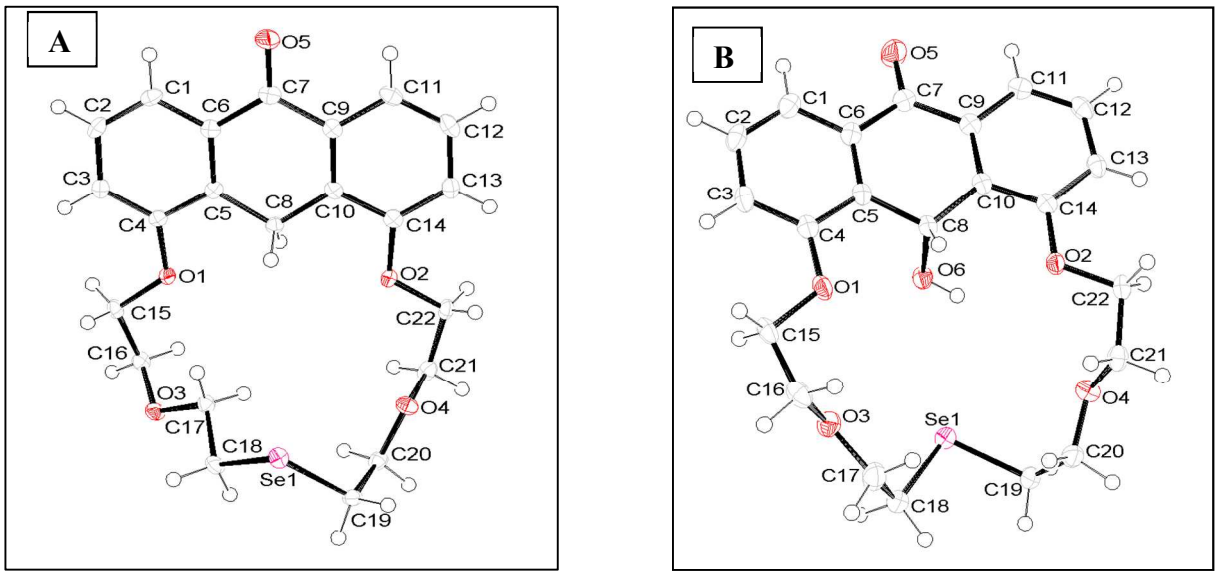

Fig. 2: A) Thermal Ellipsoid diagrams of **4**; C8-H = 1.34Å; H-C8-H = 107.9°. B) and **5**. C8-O6 = 1.445 Å; H-C8-O6 = 107.9°.

Lead Complexes: The crystal structures of the lead (II) complexes are shown in Fig. 3 and they are isostructural. The thermal ellipsoid diagrams of **7** and **8** clearly show that **2** and **3** act as tetra-dentate ligands. Pb(II) is trapped within the cavity, and the metal center possesses a distorted octahedral geometry where the axial positions are occupied by perchlorate anions (not shown). The C8-O6 bond lengths in **7** (1.229 Å) and **8** (1.236 Å) are slightly elongated after complexation with the Pb(II) ions when compared to free **2** and **3**. In complex **7** and **8**, the Pb1-O6 bond lengths are 2.600 Å and 2.604 Å respectively. These Pb-O bond lengths are consistent with our earlier reports [24, 34a]. The Pb1-S1 bond distance is 2.895 Å [34a] and the Pb1-Se1

Dalton Transactions Accepted Manuscript

bond length is 2.9904 Å, similar to earlier reported bond lengths. [34d] The bond angles S1-Pb1-O6 (161.00°) and Se1-Pb-O6 (160.92°) are slightly bent.

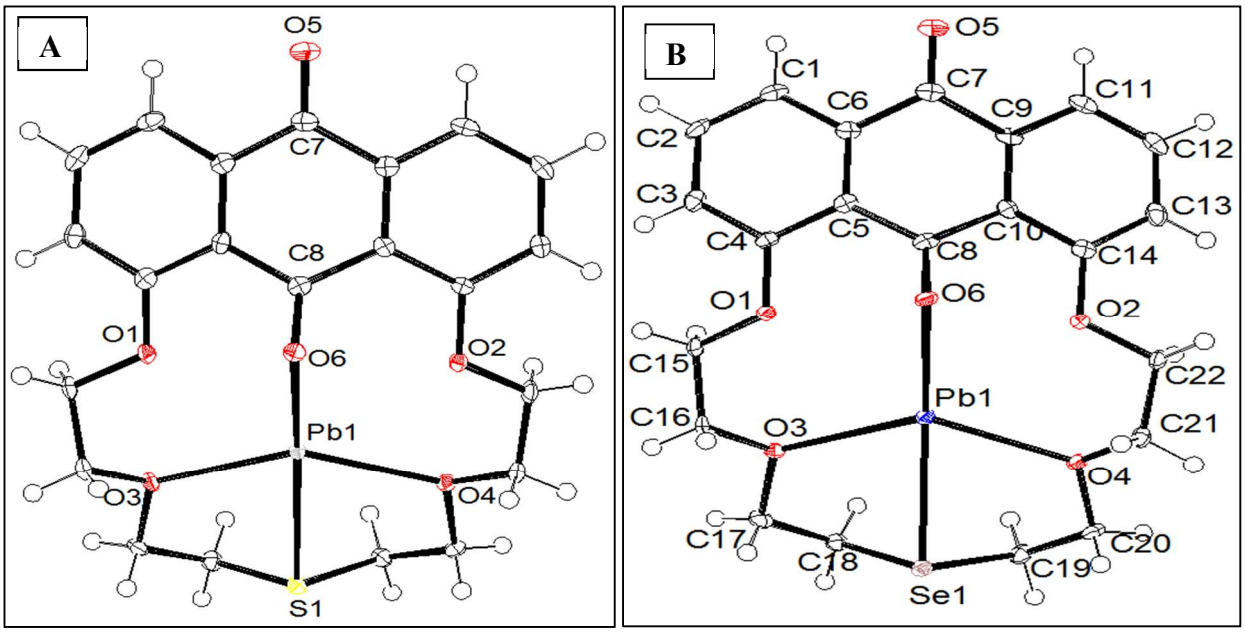

Fig.3: Thermal ellipsoid diagrams of A) [Pb(**2**)][ClO_4]$_2$, **7**: Pb1-O6 = 2.600 Å; Pb1-S1 = 2.895 Å, and B) [Pb(**3**)][ClO_4]$_2$, **8**: Pb1-O6 = 2.604Å; Pb1-Se1 = 2.9904 Å. Labels are identical except for the chalcogens for the bond angle/bond length comparison. Anions are not shown for clarity.

Absorption spectroscopy: The coordination of **2** and **3** with Pb(II) ion in solution were examined by absorption and luminescence spectrometric titrations using 1.0 x 10^{-4} molar ligand solutions in acetonitrile. The absorption spectrum of **2** exhibits a well resolved band at 380 nm, and Figure 4A is the experimental UV-visible titration curve of **2** with 0 to 2.4 equivalents of Pb(II) ion. In the presence of Pb(II), the band at 380 nm undergoes a small red shift with a clean isobestic point indicating the formation of the **2**-Pb(II) complex. The presence of other metal ions did not change the absorption spectrum of **2** appreciably (SI Fig. 16A), except for the addition of Fe(III) which caused a slight blue shift that may be due to the oxidation of sulfide in **2** in to sulfoxide (SI Fig. 26-27). Similarly, the addition of Pb(II) to **3** in acetonitrile resulted in the same red shift (Fig. 4B) and the formation of an isobestic point. Again, little change was

Dalton Transactions Accepted Manuscript

observed in the presence of other metal ions (SI Fig. 8B), and the addition of Fe(III) caused a blue shift, which may be attributed to the oxidation of selenide in **3** in to selenoxide. Redox chemistry of sulfide/ selenide in to sulfoxide/selenoxide made new host molecules, and they are the subjects of another paper.

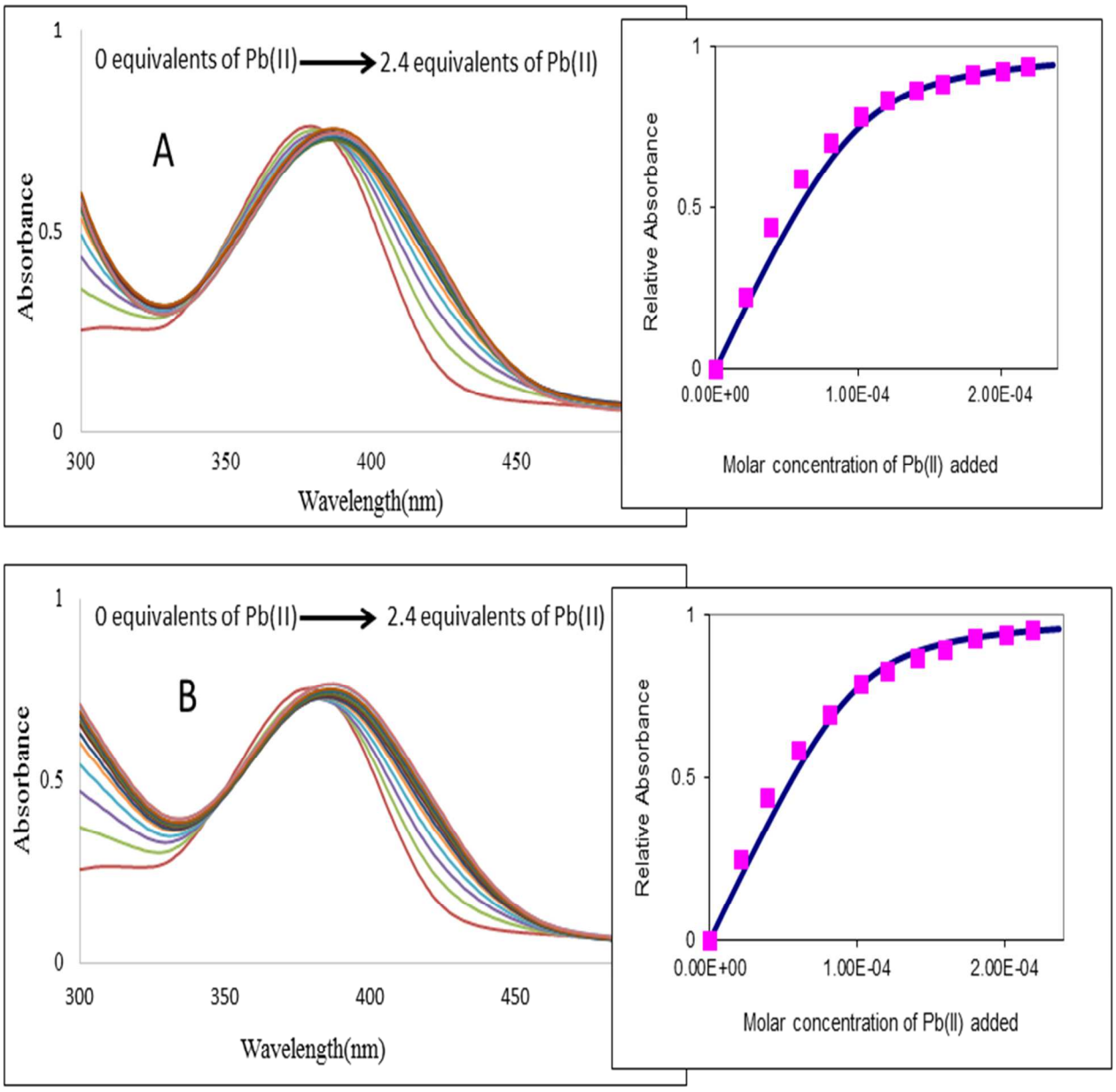

Fig. 4: Absorbance of **2** (A) and **3** (B) with aliquots of Pb(II). Inset shows the relative absorbance at 425 nm vs equivalents of Pb(II) added. $1x10^{-4}$ Molar of **2** and **3** in acetonitrile was used.

Dalton Transactions Accepted Manuscript

Luminescence spectroscopy: The emission spectrum of **2** in acetonitrile was recorded after excitation at 390 nm. Free **2** is weakly emissive and has almost no emission at 520 nm; however adding successive amounts of Pb(II) induces an increase in the emission at 520 nm by ~12.3 fold.

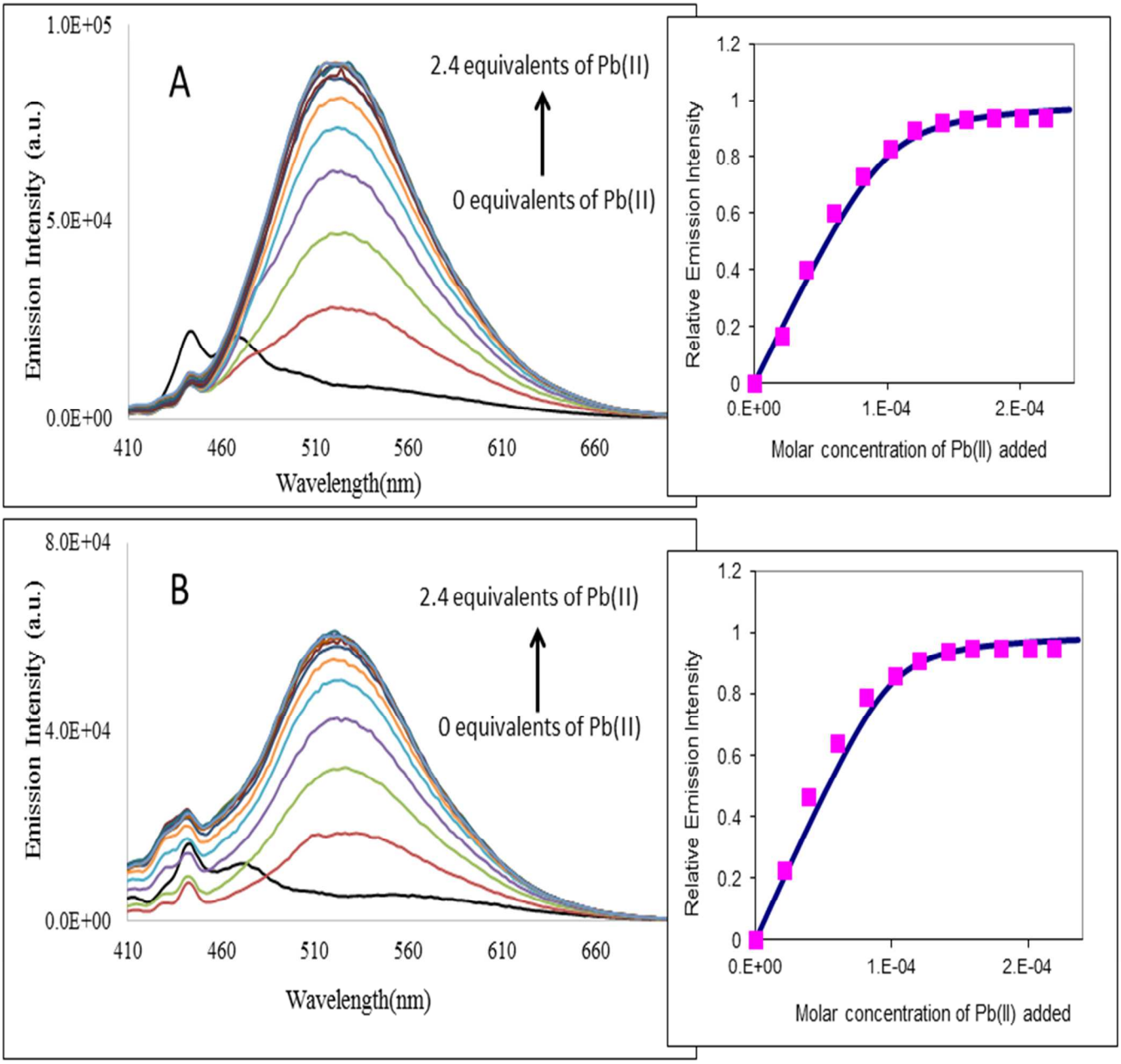

Fig.5: Emission titration of **2** (A) and **3** (B) with Pb(II). Inset shows the best fit of emission relative intensity at 520 nm vs equivalents of Pb(II) added. 1.0 x10^{-4} molar of **2** and **3** in acetonitrile was used and the excitation wavelength = 390 nm.

Dalton Transactions Accepted Manuscript

The interaction between **2** and lead ion is immediate even with 0.2 equivalent of Pb(II). Figure 5A illustrates the enhancement of the emission intensity of **2** with different equivalents of added Pb(II) ions, and the inset is the plot of relative emission intensity at 520 nm against the equivalents of Pb(II) added. It is clear from the inset plot the emission intensity reaches a plateau after addition of 1.0 equivalent of Pb(II) ions and that there is no substantial enhancement of the emission intensity upon the further addition of Pb(II), which supports the formation of a 1:1 **2**-Pb(II) complex. There is no significant change in the emission upon the addition of other metal ions to the solution of **2** (SI Fig. 17), and since lead caused a noticeable enhancement in luminescence at 520 nm, **2** is clearly selective towards Pb(II). Similar changes were observed when **3** was mixed with Pb(II). The enhancement in emission at 520 nm is even larger, ~18 fold (Fig. 5B). The addition of Cu(II) to **3** causes a red shift in the UV-visible spectrum, but did not produce any luminescence. As with compound **2**, **3** selectively senses Pb(II) as no change in luminescence was observed upon the addition of other metal ions (SI Fig. 18). However, compound **6** does not produce enhanced emission with Pb(II); although, with addition of Ca(II) and Mg(II), the emission is turned on, but only minimally (SI Fig. 19). This difference in selectivity may be due to the size of the cavity in **6** as well as the softness of tellurium. As the size of the donor atom increases from oxygen to tellurium, this may lead to a smaller cavity size in **6** and result in the inability to bind larger cations such as Pb(II) within the macrocycle. Emission is observed for smaller cations but is not particularly selective. Several attempts were made to isolate X-ray-quality crystals of **6** and its complexes, but they were unsuccessful.[45] Figure 6 also compares the luminescence intensity for all four anthraquinone-18-crown-5 derivatives.

Dalton Transactions Accepted Manuscript

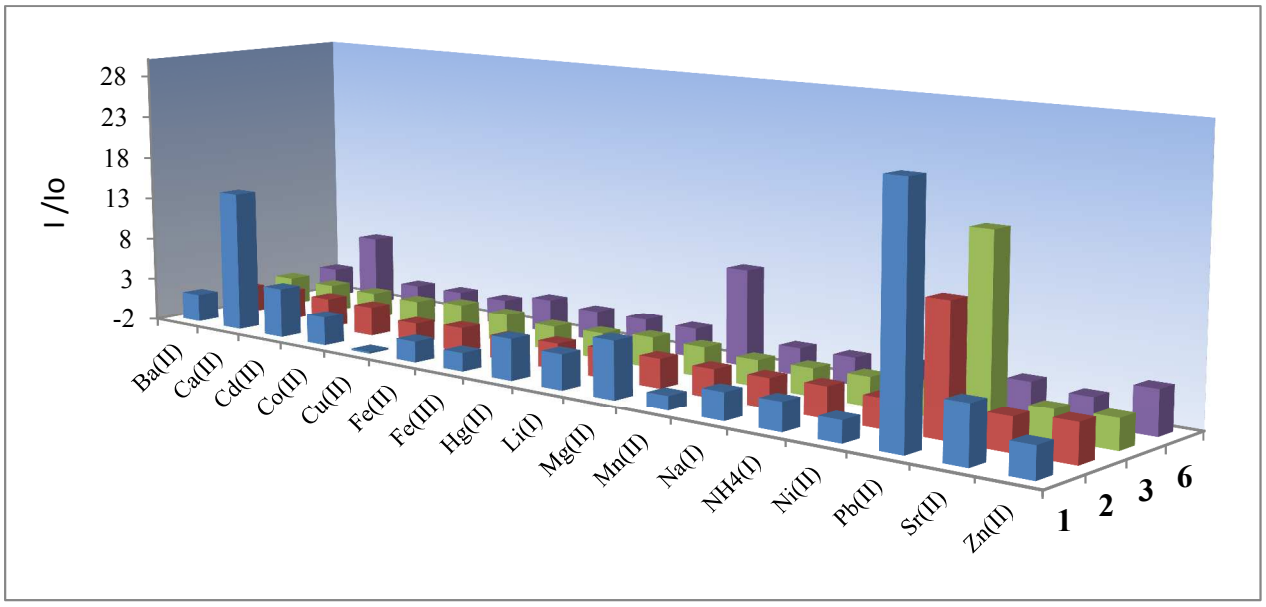

Fig. 6: Relative emission intensities at 520 nm of **1**, **2**, **3** and **6** ($1x10^{-4}$ molar in CH_3CN) with 2 equivalents of series of cations. 390 nm was used as excitation wavelength.

Binding constants were obtained by curve fitting the titration data as per our earlier report.[24] The average binding constants of **2** and **3** with Pb(II) are $1.6x10^5$ M^{-1} and $2.3x10^5$ M^{-1}, respectively, which is smaller than the binding constant determined originally for **1** with Pb(II) ($3.2x10^5$ M^{-1}).[24] We attribute the smaller binding constant to the softer sulfur and selenium donor atoms in **2** and **3**. A very similar result was observed in the lifetime experiments. Lifetime data for **2** with Pb(II) showed a single exponential decay. Both phase plane methods[46] and curve simulations[47] gave lifetime of 1/10 of a ns, whereas the lifetime of **1** with Pb(II) is 0.5 ns. **3**'s lifetime with Pb(II) is very similar (0.1 to 0.2 ns) to that of **2** with Pb(II).

Competition Studies

A competition study was performed to show the selectivity of **2** and **3** for Pb(II) in acetonitrile in the presence of other metal cations. SI Figure 20 shows the normalized relative emission intensity at 520 nm of **2** or **3** with lead and added metal ions; the graph clearly shows that the

Dalton Transactions Accepted Manuscript

other metal ions did not affect the selectivity of **2** or **3** towards Pb(II). We observed that among the metal ions studied, only Pb(II) metal ions change the emission behavior of **2** and **3**.

Theoretical Calculations

Fukui et al. [48a] were the first to define the reactivity and the stability of a molecule by means of determining energies of the highest occupied molecular orbital (HOMO) and lowest unoccupied molecular orbital (LUMO). The energy of the HOMO can determine a molecule's electron donating and accepting ability. The energies of calculated frontier molecular orbitals are given in Table 3. Soft bases will have a HOMO of higher energy than the HOMO energy of hard bases, which is also reflected in this work.[48d] From the table 3, The HOMO level of **1** is lower in energy than the HOMO level of the tellurium analog **6** which clearly indicates that **1** is a lithophile and **2** and **3** are chalcophiles. Furthermore, an examination of the molecular orbitals contributing to the lowest energy absorbance peak suggests that during excitation, electron density is transferred from the ether oxygens at the 1,8 positions of the anthraquinone to the carbonyl oxygens (SI Fig. 21). In the presence of Pb(II), this internal charge transfer process is stabilized by lowering the energy of the LUMO, resulting in a red shift in the predicted absorbance (SI Fig. 22).

The optimized structure for **6**; **6**+Pb(II); **6**+Mg(II) are given in Fig. 7 as well as the frontier molecular orbitals of **6**. Compound **6** was also optimized with Pb(II) as well as with Mg(II). Conformation for **6** with Pb(II) is bent (Fig. 7D) with a bond angle for Te-Pb-O=C measures as 93.8° in optimized structure; whereas S-Pb-O=C and Se-Pb-O=C in **7** and **8** are measured as 161.00° and 160.92°, respectively in X-ray crystallography. The computationally determined infrared stretching frequencies of the internal C=O bond increase as the heteroatom size increases. This C=O bond theoretically absorbs at 1534.93 cm^{-1} for **2**-Pb(II), 1536.81 cm^{-1} for **3**-

Dalton Transactions Accepted Manuscript

Pb(II), and 1537.37 cm^{-1} for **6**-Pb(II) (SI Fig. 23). Tables of atom coordinates and absolute energies for **1**, **2**, **3**, **6**, **6** with Pb(II) and **6** with Mg(II) are available as supporting information.

Table 3: Energies of the HOMO and the LUMO for **1**, **2**, **3** and **6**.

Compounds	**HOMO**	**LUMO**	**HOMO:LUMO gap**
	LanL2DZ (eV)	LanL2DZ (eV)	LanL2DZ (eV)
1	-6.6426	-3.1851	3.4575
2	-6.1955	-3.2463	2.9492
3	-5.9152	-3.1826	2.7326
6	-5.5696	-3.1767	2.3930
6+Pb(II)	-7.2029	-4.1008	3.1021
6+Mg(II)	-6.7781	-4.0371	2.7410

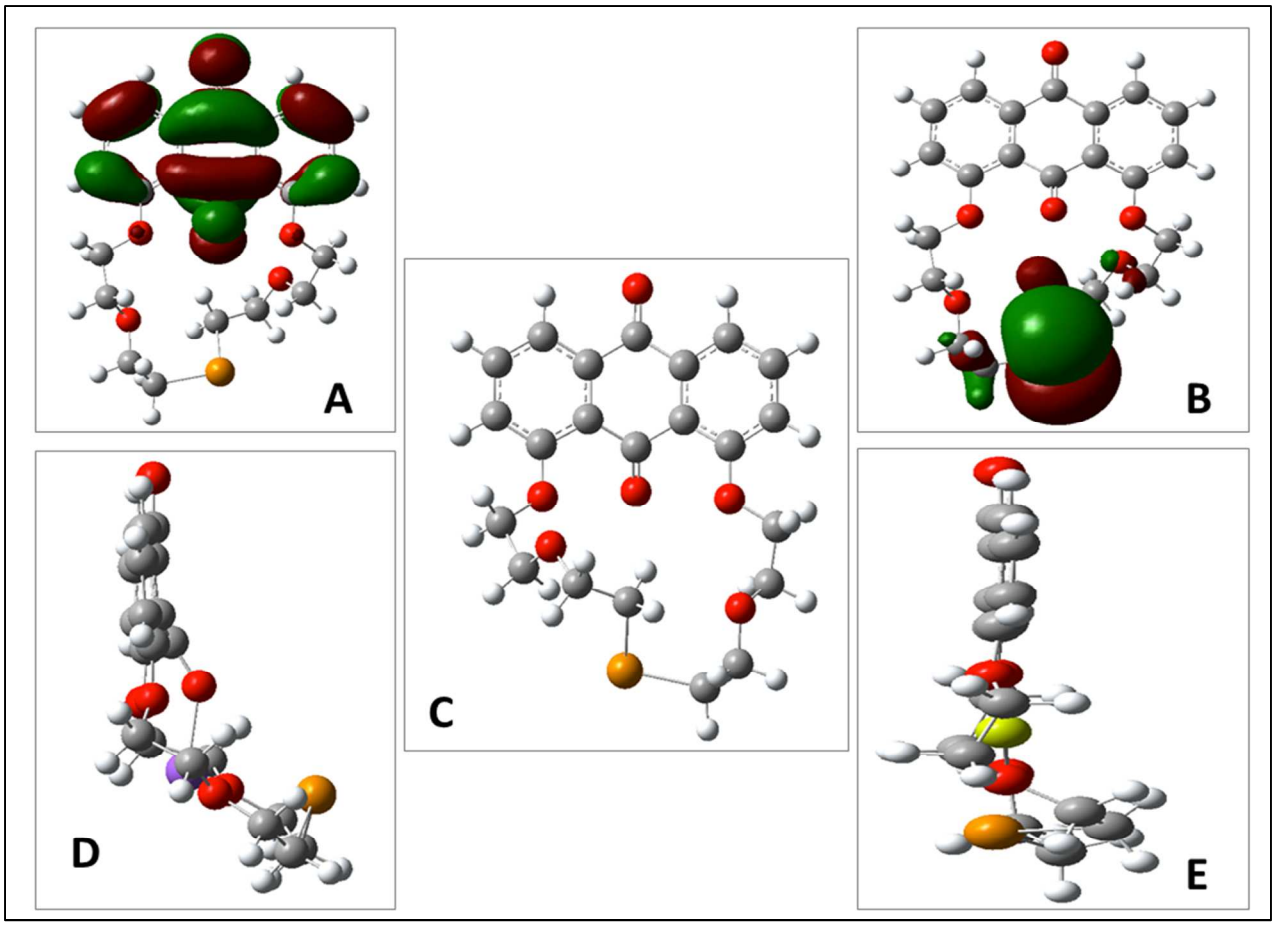

Fig. 7: A) HOMO of **6**; B) LUMO of **6**; C) Optimized geometry of **6**; D) Optimized geometry of **6**+Pb(II); E) Optimized geometry of **6**+Mg(II).

Dalton Transactions Accepted Manuscript

Table 4: Electrochemical data

Compound	Solvent	$E^{A}_{1/2}$ (V)		
		Anthraquinone$^{0/-1}$	Anthraquinone$^{-1/-2}$	Chalcogen's Oxidation
1	CH_3CN	-1.06	-1.40	Not observed
2	CH_3CN	-1.07	-1.52	+1.47^{B}
3	CH_3CN	-1.07	-1.51	+1.25^{B}
4	CH_3CN	-	-1.79^{B}	+1.21^{B}
5	CH_3CN	-	-1.60^{B}	+1.10^{B}
6	CH_3CN	-1.06	-1.57	+0.87^{B}
7	CH_3CN	-	-	+1.31^{B}
8	CH_3CN	-	-	+0.95^{B}

1. All measurements were done at room temperature
2. Only a positive scan was performed for **7** and **8**.
3. A: Referenced vs. Ag/AgCl, glassy carbon, 1mM in 0.1M tetrabutylammonium perchlorate
4. B: Irreversible

Cyclic voltammetry

Cyclic voltammetric measurements were carried out in a 0.1 M tetrabutylammonium perchlorate solution with CH_3CN as solvent vs Ag/AgCl as the reference electrode. E^{o} values for the different anthraquinone derivatives and are listed in Table 4. Compounds **2, 3,** and **6** have two typical one-electron, reversible anthraquinone reduction potentials[22, 28, 34a-c]; whereas the compounds **4** and **5** have only a single one-electron, irreversible anthraquinone reduction potentials, due to the reduction of the inner annular carbonyl group. Apart from the anthraquinone reduction potentials, **2-8** also have an irreversible oxidation peak at ~ +1.47, +1.25, +0.87 V, which is characteristic for the oxidation of S^{2-}, Se^{2-} and Te^{2-} similar to earlier reports. [34 and 49] The cyclic voltammograms of **2**, **3** and **6 (**shown in Figure 8) clearly demonstrate that the oxidation potential of the chalcogenides decreases gradually as the electronegativity of the heteroatom decreases.

Dalton Transactions Accepted Manuscript

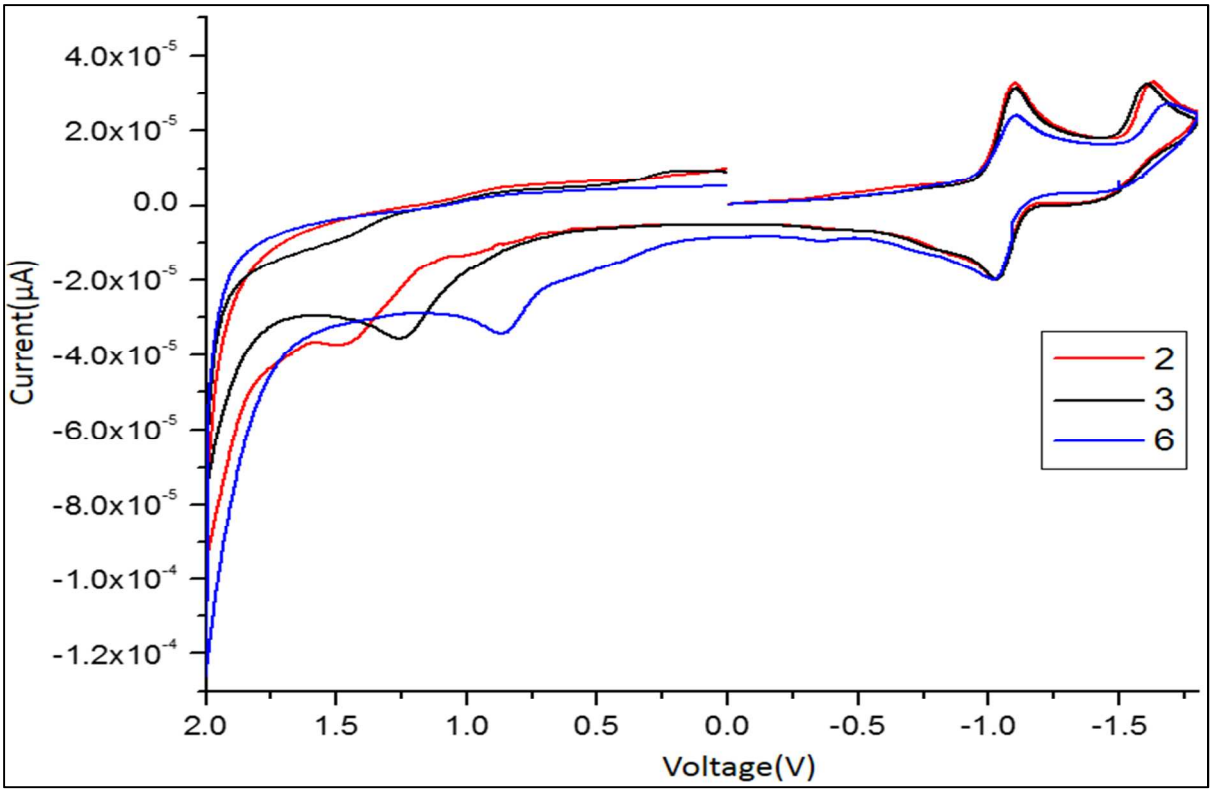

Figure 8: Cyclic voltammograms of $1x10^{-3}$ molar **2**, **3** and **6** in CH_3CN using 0.1M $TBAClO_4$ vs. Ag/AgCl on glassy carbon electrode.

For **2** and **3**, no shift is observed in the anthraquinone first and second one-electron reduction potential (E^{o1} and E^{o2}) after binding with Pb(II), but the binding of a the lead cation does cause a negative shift in the oxidation potential by ~0.2 V. This is likely due to the close proximity of the electropositive Pb(II) cation near the sulfur or selenium heteroatoms. The positive scans of **7** and **8** are given in SI Fig. 24.

Discussion

In compounds **2** and **3**, the anthraquinone acts as the lumophore and the polyether chain macrocycle binds the metal ion within the cavity. The metal center makes coordinate covalent bonds with the donor atoms in the polyether chain as well as with the inner carbonyl group of the anthraquinone, which is essential for luminescence enhancement to occur. We attribute the

Dalton Transactions Accepted Manuscript

enhancement of emission intensity for **2** and **3** upon complexation with Pb(II) is due to an internal charge transfer[7] process. For compounds **2** and **3**, the polyether chain receptor is integrated with anthraquinone fluorophore and there is charge transfer within the anthraquinone lumophore upon complexation with the Pb(II) cation with resulting enhancement in luminescence at 520 nm. The identity of the donors in the polyether chains, the cavity size, and the charge/size ratio of the cation all determine the selectivity and intensity of the luminescence of these AQ-based sensors. [26 and 27] The polyether chain in compound **1** contains oxygen as a donor atom which is a hard base; hence emission is enhanced in presence of hard acids and oxophillic metal ions. [23 and 24] Replacing two or more oxygen by sulfurs at the chelating positions cause **1** changes the selectivity of these related macrocycles towards Cd(II) and Hg(II). [26] However, in compounds **2**, **3** and **6**, the oxygen atom farthest from the inner annular carbonyl group in **1** has now been replaced by sulfur, selenium and tellurium. This change is sufficient to reduce the hardness of the polyether chain in **1**, which is reflected in the emission spectra of **2**, **3** and **6** with different metal ions. Figure 6 compares the relative luminescence intensity for all four O, S, Se, and Te anthraquinone-18-crown-5 derivatives. Alkaline earth metal cations such as Ca(II) and Mg(II), which previously caused luminescence enhancement for the oxygen analogue **1**, show almost no emission enhancement for **2** and **3**, and this may be attributed to the substitutions by the soft donors sulfur and selenium. Pb(II) prefers sulfur or selenium as donors over oxygen, and this fact is confirmed comparing Pb1-O6 bond lengths. The Pb1-O6 bond length is lengthier in $[Pb.\mathbf{2}]^{2+}$ (2.60 Å) and $[Pb.\mathbf{3}]^{2+}$ (2.62 Å) than Pb-O6 in $[Pb.\mathbf{1}]^{2+}$ (2.58 Å) complex, and this elongation in bond length may be due to the *trans* influence. The strength of coordinate covalent bond between the inner carbonyl in **2** or **3** with Pb(II) is fundamental for the luminescence intensity. The interaction between the carbonyl oxygen in **1** and Pb(II) is stronger

Dalton Transactions Accepted Manuscript

than this interaction in **2** or **3** with Pb(II). The longer bond length (Pb-O6) indicates a weaker interaction between Pb(II) and the carbonyl oxygen in **7** or **8,** may be which explains the lower luminescence intensity of **7** and **8** compared to lead complex of **1**. Replacing oxygen with other donors in the polyether chain reduces the emission intensity (SI Fig. 25) drastically when perchloric acid generated hydronium ion binds within the cavity. This also supports that **2**, **3** and **6** are softer bases than **1** even though the binding sites for the hydronium ion are identical.

Conclusion

In summary, anthraquinone-based receptors **2** and **3** are luminescent sensors for the selective recognition of Pb(II) in acetonitrile via internal charge transfer. We have demonstrated that by changing the identity of a single donor atom in the polyether chain of **1,** the selectivity towards Pb(II) is increased. Compounds **2** and **3** form a 1:1 (M:L) complex with Pb(II) ions in the solid-state and in an acetonitrile solution, which are confirmed by spectroscopic titrations and X-ray crystallography. Complexation of **2** or **3** with Pb(II) causes enhancement in emission at 520 nm; whereas compound **6** does not appear to bind heavy metal ions, hence it does not show a change in luminescence with added Pb(II). Furthermore, compounds **2** and **3** show significant changes in sulfur and selenium oxidation potentials after coordination with Pb(II). We have also used DFT calculations to confirm that the expected hardness of the ligands decreases in the following order: **1** > **2** > **3** > **6**.

Experimental section

^{1}H and ^{13}C NMR spectra were obtained using Varian 200 MHz and Bruker 400 MHz instruments at room temperature using deuterated solvents. Absorbance data was collected using a Varian Cary 50 BIO UV-Visible spectrophotometer. Luminescence titrations were conducted using a Fluoromax–4 spectrofluorometer. Mass spectrometry was conducted using a Varian 500-MS IT ESI mass spectrometer. Cyclic voltammograms were recorded using a CH instruments 660

Dalton Transactions Accepted Manuscript

electrochemical workstation. Elemental analyses were conducted using an Exeter CE-440 Elemental analyzer. Melting points were determined using open capillaries and were uncorrected.

Chemicals and reagents

1,8-Oxybis(ethyleneethoxyethyleneethoxy)anthracene-9,10-dione (**1**)[22] and 1,8-bis(2-bromoethylethyleneoxy)anthracene-9,10-dione[54] were synthesized using available procedures. Sodium sufide nonahydrate, selenium as powder, tellurium as powder, sodium borohydride, tetrabutylammonium perchlorate (TBAP) and all metal perchlorate salts were purchased from Aldrich, and used without purification. The perchlorate salts used in selectivity studies were dried at 100 °C under vacuum over Driete to minimize the effects of hydration. CH_3CN, THF, DMF and CH_2Cl_2 were purchased from Aldrich and purified using a PURE SOLV^{TM} solvent purification system. HPLC grade anhydrous acetonitrile (Fisher/Acros) was used in all spectroscopic studies. *Caution: Although we have experienced no difficulties with these perchlorate salts, they should be treated as potentially explosive and handled with care.*

Synthesis of 1, 8-oxybis(ethyleneethoxyethylenethio)anthracene-9,10-dione (2):

1,8-bis(2-bromoethoxy)anthracene-9,10-dione (0.50 g, 0.92 mmol), which was made in 40 mL of THF, was stirred in a round bottom flask under N_2 atmosphere. Sodium sulfide nonahydrate (0.22 g, 0.92 mmol) was dissolved in 10 mL of DI water and added to the round-bottom flask in drop-wise. The solution was stirred for three hours with mild heating. The reaction mixture was cooled to room temperature, mixed with 200 mL of distilled water and extracted with CH_2Cl_2. The organic layer was dried with anhydrous Na_2SO_4. Most of the solvents were evaporated under reduced pressure, and a silica gel column using ethyl acetate as eluent was used to purify the compound. A yellow solid was obtained. The yield is 0.25 g (65%) and the melting point is 174

Dalton Transactions Accepted Manuscript

– 178 °C. Elemental analyses calculated for $C_{22}H_{22}O_6S$: C, 63.75; H, 5.35; S, 7.74 %. Found: C, 63.58; H, 5.32; S, 7.29 %. ^{1}H NMR (at 25 °C, $CDCl_3$): δ 2.85 – 2.92 (*t*, 4H, CH_2-S); 3.97 – 4.03 (*m*, 8H, CH_2-O); 4.22 – 4.26 (*t*, 4H, CH_2-O); 7.19 – 7.25 (*m*, 2H, ArH); 7.55 – 7.63 (*t*, 2H, ArH); 7.80 – 7.85 (*d*, 2H, ArH). ^{13}C NMR (at 25 °C, $CDCl_3$): δ 31.8, 68.9, 70.2, 72.4, 118.2, 119.2, 124.4, 133.7, 134.8, 158.4, 181.8, 184.0.

Synthesis of 1, 8-oxybis(ethyleneethoxyethyleneseleno)anthracene-9,10-dione (3):

0.14 gram (1.7 mmol) of selenium powder was mixed with 50 mL of 95% ethanol and warmed under nitrogen atmosphere. Sodium borohydride (0.14 g in 5 mL of 1M NaOH) was added in aliquots until the solution become colorless (*Excess of $NaBH_4$ will decrease the yield of **3***). 1,8-bis(2-bromoethoxy)anthracene-9,10-dione (0.95 g, 1.7 mmol), which was made in 20 mL of THF was added and the solution was stirred for three hours with gentle heating. The reaction mixture was cooled to room temperature, mixed with 200 mL of distilled water and extracted with CH_2Cl_2. The organic layer was dried with anhydrous Na_2SO_4. Most of the solvents were evaporated under reduced pressure. A thin layer chromatogram showed that there are three compounds, and a silica gel column with methylene chloride: ethyl acetate as eluent was used to separate them. **3** is obtained as a yellow solid. The yield is 0.2 gram (25% yield), and the melting point is 180 – 182 °C. Elemental analyses calculated for $C_{22}H_{22}O_6Se$: C, 57.27; H, 4.81 %. Found: C, 57.18; H, 4.78 %. ^{1}H NMR (at 25 °C, $CDCl_3$): δ 2.88 – 2.93 (*t*, 4H, CH_2-Se); 3.99 – 4.10 (*m*, 8H, CH_2-O); 4.22 – 4.26 (*t*, 4H, CH_2-O); 7.21 – 7.25 (*m*, 2H, ArH); 7.55 – 7.63 (*t*, 2H, ArH); 7.80 – 7.85 (*d*, 2H, ArH). ^{13}C NMR (at 25 °C, $CDCl_3$): δ 23.3, 68.9, 70.3, 72.9, 118.9, 119.2, 133.7, 134.8, 158.4, 182.0.

Dalton Transactions Accepted Manuscript

1, 8-oxybis(ethyleneethoxyethyleneseleno)-10-dihydraanthracene-9-one (4):

Compound **4** obtained as a pale yellow solid eluted by methylene chloride while isolating compound **3**. The yield is 0.3 g (38%), and the melting point is 210 – 212 °C. *Compound **4** can be prepared by refluxing **3** with 1 equivalent of $NaBH_4$ in ethanol for 3 hour.* Elemental analyses calculated for $C_{22}H_{24}O_5Se$: C, 59.06; H, 5.41 %. Found: C, 58.68; H, 5.25 %.

^{1}H NMR (at 25 °C, $CDCl_3$): δ 2.88 – 2.92 (*m*, 4H, CH_2-Se); 3.94 – 3.98 (*m*, 8H, CH_2-O); 4.18 (*s*, 2H, anthrone proton); 4.25 – 4.27 (*m*, 4H, CH_2-O); 7.06 – 7.09 (*d*, 2H, ArH); 7.37 – 7.42 (*t*, 2H, ArH); 7.97 – 7.99 (*d*, 2H, ArH). ^{13}C NMR (at 25 °C, $CDCl_3$): δ 22.7, 23.8, 68.7, 69.2, 72.6, 114.1, 119.4, 127.2, 130.3, 132.7, 156.0, 181.8.

1, 8-oxybis(ethyleneethoxyethyleneseleno)-10-hydroxy-10-hydro-anthracene-9-one (5):

Compound **5** obtained as a cream color solid eluted by methylene chloride and ethyl acteate mixture while separating **3** by column chromatography. The yield is 0.1 g (12%), and the melting point is 206 – 209 °C. *Compound **5** can be prepared by stirring **3** with 1 equivalent of $NaBH_4$ in ethanol for 30 minute at room temperature.* Elemental analyses calculated for $C_{22}H_{24}O_6Se$: C, 57.02; H, 5.22 %. Found: C, 57.07; H, 5.18 %. ^{1}H NMR (at 25 °C, $CDCl_3$): δ 2.86 – 2.95 (*m*, 4H, CH_2-Se); 3.87 – 3.99 (*m*, 8H, CH_2-O); 4.27 – 4.36 (*m*, 4H, CH_2-O); 4.47 (bs, 1H, OH); 6.41 (*s*, 1H, CH); 7.14 – 7.17 (*d*, 2H, ArH); 7.42 – 7.46 (*m*, 2H, ArH); 7.88 – 7.90 (*d*, 2H, ArH). ^{13}C NMR (at 25 °C, $CDCl_3$): δ 23.1, 57.2, 68.9, 69.1, 72.2, 117.0, 119.9, 129.2, 131.7, 132.3, 156.9, 184.9.

Synthesis of 1, 8-oxybis(ethyleneethoxyethylenetelluro)anthracene-9,10-dione (6):

0.15 gram (2.2 mmol) of tellurium powder and 1,8-bis(2-bromoethoxy)anthracene-9,10-dione (1.00 g) were used to synthesize **6** using a procedure identical to that used to make **3**. Compound **6** was purified by silica gel column using a CH_2Cl_2:CH_3OH (18:2) mixture as an eluent. A

Dalton Transactions Accepted Manuscript

yellow colored solid was obtained. The yield is 0.1 g (10%), and the melting point is 172 – 175 °C. Elemental analyses calculated for $C_{22}H_{22}O_6Te$: C, 51.81; H, 4.35 %. Found: C, 51.90; H, 4.28 %. ESI MS: 533.01 (Calc. for **6** with Na^+), 533.35 (found). ^{1}H NMR (at 25 °C, $CDCl_3$): δ 2.89 – 2.96 (*t*, 4H, CH_2-Se); 3.99 – 4.03 (*m*, 4H, CH_2-O); 4.09 – 4.17 (*t*, 4H, CH_2-O); 4.23 – 4.27 (*m*, 4H, CH_2-O); 7.20 – 7.25 (*m*, 2H, ArH); 7.55 – 7.63 (*t*, 2H, ArH); 7.80 – 7.84 (*d*, 2H, ArH). ^{13}C NMR (at 25 °C, $CDCl_3$): δ 2.4, 68.9, 70.3, 74.4, 119.0, 119.2, 124.6, 133.7, 134.9, 158.5, 181.8, 184.0.

Synthesis of [Pb.2](ClO$_4$)$_2$ (7)

Lead (II) perchlorate trihydrate (0.11 g, 0.24 mmol), which was dissolved in 10 mL of acetonitrile was added in aliquots with a solution of **2** (0.1 g, 0.24 mmol) made in 20 mL of acetonitrile. The solution was stirred for 2 h and then was evaporated under reduced pressure. The entire residue was dissolved in 10 mL of CH_3CN:CH_3OH (8:2), and diethylether was diffused into the solution. Fine yellow blocks were obtained. Yield: 0.135 g (70% as crystals) and it decomposes over 210 °C. Elemental analyses calculated for $C_{22}H_{22}O_{14}SPbCl_2$: C, 32.19; H, 2.68; S, 3.91%. Found: C, 32.16; H, 2.75; S, 3.75 %. ^{1}H NMR (CD_3CN, 25 °C): δ 3.21 – 3.33 (*m*, 4H, CH_2-S); 4.02 – 4.18 (*m*, 8H, CH_2-O); 4.32 – 4.41 (*t*, 4H, CH_2-O); 7.38 – 7.48 (*m*, 2H, ArH); 7.72 – 7.80 (*m*, 4H, ArH). ^{13}C NMR (CD_3CN, 25 °C): δ 32.9, 69.4, 70.6, 71.5, 120.9; 121.6; 135.4; 135.7 and 158.9. (We could see the methylene carbons and few aromatic carbons due to solubility issue)

Synthesis of [Pb.3](ClO$_4$)$_2$ (8)

Lead (II) perchlorate trihydrate (0.05 g, 0.11 mmol), which was dissolved in 10 mL of acetonitrile was added in aliquots with a solution of **3** (0.049 g, 0.11 mmol) made in 20 mL of acetonitrile. The solution was stirred for 2 h and then was evaporated under reduced pressure.

Dalton Transactions Accepted Manuscript

The entire residue was dissolved in 10 mL of CH_3CN, and ether was diffused into the solution. Fine needle-shaped crystals were obtained. Yield: 0.05 g (55% as crystals) and the melting point is 170 – 172 °C (dec). Elemental analyses calculated for $C_{22}H_{22}O_{14}SePbCl_2$: C, 30.45; H, 2.53 %. Found: C, 30.55; H, 2.50 %. ^{1}H NMR (CD_3CN, 25 °C): δ 3.24 – 3.34 (*m*, 4H, CH_2-Se); 4.02 – 4.20 (*m*, 8H, CH_2-O); 4.32 – 4.44 (*t*, 4H, CH_2-O); 7.41 – 7.52 (*m*, 2H, ArH); 7.72 – 7.86 (*m*, 4H, ArH). ^{13}C NMR (CD_3CN, 25 °C): 26.8, 69.5, 70.5, 71.5, 120.7; 121.4; 135.7. (We could see the methylene carbons and a few aromatic carbons due to solubility issues)

Methods:

Crystallography: X-ray quality crystals of compounds **2** and **3** were obtained by slow evaporation of a methylene chloride solution; **4** and **5** were obtained by diffusing diethyl ether into CH_2Cl_2:CH_3OH (8:2). Crystals of **7** was obtained by diffusing diethyl ether into CH_3CN:CH_3OH (8:2). Crystals of **8** and was obtained by diffusing diethyl ether into CH_3CN. Crystallographic data for **2**, **3**, **4**, **5**, **7**, and **8** were collected at 100 K using a Bruker SMART APEX II diffractometer by MoK_α radiation. The data reduction and refinement were completed using the WinGX suite of crystallographic software. [50 and 51] Structures were solved using SIR97.[52] Both SIR97 and OLEX were used to solve **8**.[53] All hydrogen atoms were placed in ideal positions and refined as riding atoms with relative isotropic displacement parameters. Table 1 lists additional crystallographic and refinement information. The polyether chain in **2** was modeled as disordered over two positions 50:50. Compound **8** formed as a twin crystal (30:70). One of the carbonyl group in compound **3** was modeled as disorder over two positions 65:35.

Computation: The ground states of **1**, **2**, **3**, and **6** with and without Pb(II) and **6** with Mg(II) were optimized using density functional theory (DFT)[48a] with Becke's three parameter Lee-Yang-Parr (B3LYP)[48b,c] exchange-correlation functionals and the LanL2DZ basis set.[48d,e] All ligands and

Dalton Transactions Accepted Manuscript

complexes were assumed to be in a singlet state during optimization. The initial atomic coordinates of the ligands with and without metal ions were derived from the single crystal X-ray diffraction structure of **2** with Pb(II). Counterions were artificially removed for all structures, and Pb(II) was removed for the optimization of the isolated ligands. The solvation by acetonitrile was modeled by the integral equation formalism polarizable continuum model (IEFPCM).[48f] TDDFT[48g] and frequency calculations were performed on the optimized structures. All of the harmonic frequencies for the optimized structures were real. 52 singlet states were solved for in the TDDFT calculations. The "state of interest" was defined as 50. Gaussian 09[48h] Software was used for all calculations. Default settings were used for all calculations unless specified above. Computations supporting this project were performed on High Performance Computing systems at the University of South Dakota.

Acknowledgements

DMJ gratefully acknowledges support from NSF-REU (CHE-106300). NSF-EPSCoR (EPS-0554609) and the South Dakota Governor's 2010 Initiative are also appreciated for the purchase of a Bruker SMART APEX II CCD diffractometer. NSF-URC (CHE-0532242) also provided funding for the purchase of the elemental analyzer. We thank Aravind Baride and Dr. P. Stanley May for nanosecond lifetime measurements.

Supporting Information Available: Crystallographic characterization data, NMR, MS, and Tables of atom coordinates with absolute energy, cyclic voltammetry, and spectroscopic data are available for free of charge.

Dalton Transactions Accepted Manuscript

References

1. (a) J. Liu, Y. Lu, Y. *J. Am. Chem. Soc.* 2004, **126**, 12298. (b) P. Chen, C. He, *J. Am. Chem. Soc.* 2004, **126**, 728. (c) D. Prabhakaran, M. Yuehong, H. Nanjo, H. Matsunaga, *Anal. Chem.* 2007, **79**, 4056.
2. (a) J. P. Taylor, J. Hardy, K. H. Fischbeck, *Science,* 2002, **296**, 1991. (b) J. W. Kelly *Curr. Opin. Struct. Biol.,* 1998, **8**, 101. (c) E. M. Sigurdsson, T. Wisniewski, B. Frangione, *Trends Mol. Med.,* 2002, **8**, 411. (d) T. Chiba, Y. Hagihara, T. Higurashi, K. Hasegawa, H. Naiki, Y. Goto, *J. Biol. Chem.,* 2003, **278**, 47016.
3. N. Castelino, P. Castelino, N. Sannolo, *Inorganic Lead Exposure: Metabolism and Intoxication*. The Agency for Toxic Substances and Disease Registry (ATSDR), U.S. Department of Health and Human Services; http:// www.atsdr.cdc.gov/, accessed on May 22, 2008; Lewis Publishers: Boca Raton, 1995.
4. F. E. McNeill, J. M. O'Meara, *Adv. X-ray Anal.*, 1999, **41**, 910.
5. (a) A. Mimendia, A. Legin, A. Merkoc-i, *M.* del Valle, *Sens. Actuators B,* 2010, **146**, 420. (b) A. Merkoc-i, S. Alegret, *Comprehensive Analytical Chemistry; Elsevier B.V.: Amsterdam,* 2007, **Chapter 49**, 143.
6. R. Niessner, *Trends Anal. Chem.,* 1991, **10**, 310.
7. X. Qian, Y. Xiao, Y. Xu,; X. Guo, J. Qian, W. Zhu, *Chem. Commun*., 2010, **46**, 6418.
8. A.P. de Silva, H.Q.N. Gunaratne, T. Gunnlaugsson, A.J.M. Huxley, P.C. McCoy, J.T. Rademacher, T.E. Rice, *Chem. Rev.,* 1997, **97**, 1515.
9. (a) V. Thiagarajan, P. Ramamurthy, D. Thirumalai, V. T. Ramakrishnan, *Org. Lett.,* 2005, **7**, 657. (b) T. Gunnlaugsson, M. Glynn, G. M. Tocci, P. E. Kruger, F. M. Pfeffer,

Dalton Transactions Accepted Manuscript

Coord. Chem. Rev., 2006, **250**, 3094. (c) A. P. de Silva, G. D. McClean, T. S. Moody, S. M. Weir, *Handb.Photochem. Photobiol.,* 2003, **3**, 217. (d) A. P. de Silva, D. B. Fox, A. Huxley, T. S. Moody, *Coord. Chem. Rev.,* 2000, **205**, 41. (e) A. P. de Silva, H. Q. N. Gunaratne, T. Gunnlaugsson, A. J. M. Huxley, C. P. McCoy, J. T. Rademacher, T. E. Rice, *Chem. Rev.,* 1997, **97**, 1515 and references within. (f) *Fluorescent Chemosensors for Ion and Molecular Recognition*; A. W. Czarnik, *Ed.; American Chemical Society: Washington, DC,* 1992. (g) K. Rurack, *Spectrochim. Acta,* 2001, **A57**, 2161.

10. (a) A. B. Othman, J. W. Lee, J.Wu, J. S. Kim, R. Abidi, P. Thuery, J. M. Strub, A. Van Dorsselaer, J. Vicens, *J. Org. Chem.,* 2007, **72**, 7634. (b) J. Fan,; M. Hu,; P. Zhan,; Z. Peng, *Chem.Soc.Rev.*, 2013, **42**, 29.
11. M. Formica, V. Fusi, L. Giorgi, M. Micheloni, *Coord.Chem.Rev*., 2012, **256**, 170.
12. (a) K. K.-W. Lo,; M.-W. Louie,; K. Y. Zhang, *Coord. Chem. Rev.,* 2010, **254**, 2603. (b) J.-C. G. Bünzli, *Chem. Rev.,* 2010, **110**, 2729. (c) T. Gunnlaugsson, T. C. Lee, R. Parkesh, *Org. Lett.,* 2003, **5**, 4065. (d) J. S. Kim, K. H. Noh, S. H. Lee, S. K. Kim, S. K. Kim, J. Yoon, *J. Org. Chem.,* 2003, **68**, 597. (e) J. S. Kim, O. J. Shon, J. A. Rim, S. K. Kim, J. Yoon, *J. Org. Chem.,* 2002, **67**, 2348.
13. N. C. Lim, J. V. Schuster, M. C. Porto, M. A. Tanudra, L. Yao, H. C. Freake, C. Bruckner, *Inorg. Chem.,* 2005, **44***,* 2018.
14. (a) Y. Wu, X. Peng, J. Fan, S. Gao, M. Tian, J. Zhao, S. Sun, *J. Org. Chem.* 2007, **72**, 62. (b) Y. Abraham, H. Salman, K. Suwinska, Y. Eichen, *Chem. Commun.* 2011, **47**, 6087.
15. S.K. Kim, J.H. Bok, R.A. Bartsch, J.Y. Lee, J.S. Kim, *Org. Lett.* 2005, **7**, 4839.
16. (a) K. Kalyanasundaram, J.K. Thomas, *J. Phys. Chem*. **1977**, *81*, 2176. (b) P. Lianos, B. Lux, D.J. Gerald, *Chim. Phys*. 1988, **77**, 907.

Dalton Transactions Accepted Manuscript

17. (a) H.-S. Bien, J. Stawitz, K. Wunderlich, *In Ullmann's Encyclopedia of Industrial Chemistry*; W. Gerhartz, Y.S. Yamamoto, F.T. Campbell, R. Pfefferkorn, J.F. Rounsaville, Eds.; VCH: Weinheim, 1985, **A2**, p. 355. (b) A.K. Mishra, J. Jacob, K. Mu¨llen, *Dyes Pigm.* 2007, **75**, 1. (c) J. F. McKellar, *Radiat. Res. Rev.,* **1971***, 3,* 141. (d) I.H. Leaver, N.S. Allen, J.F. McKeIlar, Photochemistry of *Dyed and Pigmented Polymers, Applied Science, Barking,* 1980, p. 180. (e) A.V. El'tsov, O.P. Studzinskii, U.M. Grebenkina, *Russ. Chem. Rev.,* 1977, **46**, 93. (f) G.S. Egerton, A.G. Morgan, *J. Sot. Dyers Colour*, 1971, **87**, 268. (g) J.F. McKellar, N.S. Allen, *Photochemistry of Man-Made Polymers, Applied Science, London,* 1979, Chapter 4. (h) H. Meier, K. Venkataraman, *The Chemistry of Synthetic Dyes, Academic Press, New York*, 1971, p. 389. (i) *Colour Index, Society of Dyers and Colourists, Bradford, 4th edition*, 1975. (j) K. Venkataraman, *The Chemistry of Synthetic Dyes, Vol. II, Academic Press, New York,* 1952.

18. K. A. Opperman, S.L Mecklenburg, T.J. Meyer, *Inorg. Chem.* 1994, **33**, 5295.

19. (a) L.T. Ellis, D.F. Perkins, P. Turner, T.W. Hambley, *Dalton Trans.* 2003, 2728; (b) E. Boseggia, M. Gatos, L. Lucatello, F. Mancin, S. Moro, M. Palumbo, C. Sissi, P. Tecilla, U. Tonellato, G. J. Zagotto, *J. Am. Chem. Soc.* 2004, **126**, 4543.

20. E.E. Langdon-Jones, S.J.A. Pope, *Coord.Chem.Rev.* 2014, **269**, 32.

21. (a) L. Zhu, R.F. Khairutdinov, J.L. Cape, J.K. Hurst, *J. Am. Chem. Soc.* 2006, **128**, 825–835. (b) S. Devaraj, D. Saravanakumar, M. Kandaswamy, *Tetrahedron Lett.* 2007, **48**, 3077–3081. (c) E. Ranyuk, C. M. Douaihy, A. Bessmertnykh, F. Denat, A. Averin, I. Beletskaya, R. Guilard, *Org. Lett.* 2009, **11**, 987–990.

Dalton Transactions Accepted Manuscript

22. M. Delgado, D.A. Gustowski, H.K. Yoo, V.J. Gatto, G.W. Gokel L. Echegoyen, *J. Am. Chem. Soc.* 1988, **110**, 119.

23. V.G. Young Jr., H.L. Quiring, A.G. Sykes, *J. Am. Chem. Soc.* 1997, **119**, 12477.

24. M. Kadarkaraisamy, A. G. Sykes, *Inorg. Chem.* 2006, **45**, 779.

25. M. Kadarkaraisamy, G. Caple, A.R. Gorden, A.G. Sykes, *Inorg. Chem.* 2008, **47**, 11644.

26. M. Kadarkaraisamy, A. G. Sykes *Polyhedron* 2007, **26**, 1323.

27. B. Kampmann, Y. Lian, K.L Klinkel, P.A. Vecchi, H.L. Quiring, C.C. Soh, A.G. Sykes, *J. Org. Chem.* 2002, **67**, 3878.

28. M. Kadarkaraisamy, E. Dufek, D. Lone Elk, A.G. Sykes, *Tetrahedron* 2005, **61**, 479.

29. W. Nakanishi, S. Hayashi, N. Itoh, *Chem. Commun*. 2003, 124.

30. E. Ranyuk, C.D. Morkos, A. Bessmertnykh, F. Denat, A. Averin, I. Beletskaya, R. Guilard, *Org. Lett.* 2009, **11**, 2009.

31. (a) D.Y. Han, J.M. Kim, J. Kim, H.S. Jung, Y.H. Lee, J.F. Zhang, J.S. Kim, *Tet.Lett.* 2010, **51**, 1947. (b) E. Ermakova, J. Michalak, M. Meyer, V. Arslanov, A. Tsivadze, R. Guilard, A.B. Lemeune, *Org. Lett*. 2013, **15**, 662.

32. H.J. Kim, S.H. Kim, J.H. Kim, L.N. Anh, J.H. Lee, C.H. Lee, J.S. Kim, *Tet.Lett.* 2009, **50**, 2782.

33. S.H. Kim, H.S. Choi, J. Kim, S.J. Lee, D.T. Quang, J.S. Kim, *Org. Lett.* 2010, **12**, 561.

34. (a) M. Kadarkaraisamy, D. Mukherjee, C.C. Soh, A.G. Sykes, *Polyhedron*, 2007, **26**, 4085-4092. (b) K. Mariappan, P.N. Basa, *Inorg.Chimi.Acta*, **2011**, *11*, 344-349. (c) K. Mariappan, P.N. Basa, V. Balasubramanian, S. Fuoss, A.G. Sykes, *Polyhedron*, 2013, **55**, 144-154. (d) P.A.W. Dean, J.J. Vittal, N.C. Payne, *Inorg.Chem.* 1984, **24**, 4232-4236.

Dalton Transactions Accepted Manuscript

35. K. Schwarz, C.M. Foltz, *J. Am. Chem. Soc.* 1957, **79**, 3292.

36. (a) A.J. Mukherjee, S.S. Zade, H.B. Singh, R.B. Sunoj, *Chem.Rev.* 2010**, 110**, 4357. (b) K.C. Nicolaou, N.A. Petasi, *Selenium in Natural Products Synthesis; CIS: Philadelphia,* 1984. (c) S. Patai, Z. Rappoport, *The Chemistry of Organic Selenium and Tellurium Compounds; Wiley: New York,* 1986. (d) T.G. Back, *Organoselenium Chemistry: A Practical Approach; Oxford University Press: Oxford,* 1999. (e) G. Mugesh, W.W. du Mont, H. Sies, *Chem. Rev.* 2001, **101**, 2125. (f) C.W. Nogueira, G. Zeni, J.B.T. Rocha, *Chem. Rev.* 2004, **104**, 6255.

37. (a) G. Mugesh, A. Panda, H.B. Singh, N.S. Punekar, R.J. Butcher, *J. Am. Chem. Soc.* 2001, **123**, 839. (b) K. Selvakumar, P. Shah, H.B. Singh, R.J. Butcher, *Chem. Eur. J.* 2011, **17***,* 12741. (c) B.K. Sarma, G. Mugesh, *J. Am. Chem. Soc.* 2005, **127**, 11477. (d) V. Nascimento, E.E. Alberto, D.W. Tondo, D. Dambrowski, M.R. Detty, F. Nome, A.L.J. Braga, *Am. Chem. Soc.* 2012, **134**, 138. (e) R. M. Gai, R.F. Schumacher, D.F. Back, G. Zeni, *Org. Lett.* 2012, **14**, 6072.

38. (a) A.K. Singh, S. Sharma, *Coord. Chem. Rev.* 2000, **209**, 49-98. (b). W. Levason, S.D. Orchard, G. Reid, *Coord. Chem. Rev.* 2002, **225**, 159. (b) W. Levason, G. Reid, W. Zhang, *Dalton Trans.* 2011, **40**, 8491. (c) A. Panda, *Coord. Chem. Rev.* 2009, **253**, 1056-1098. (d) A. Panda, *Coord. Chem. Rev.* 2009, **253**, 1947-1965. e) P.O. Brien, N.L. Pickett, *Comprehensive Coordination Chemistry II, ed. J.A. McCleverty, T.J. Meyer, Elsevier, Oxford,* 2004, **9**, 1005.

39. (a) J. Ahrens, B. Böker, K. Brandhorst, M. Funk, M. Bröring, *Chem.Eur. J.* 2013, **19**, 11382. (b) A.P. Singh, K.M. Lee, D.P. Murale, T. Jun, H. Liew, Y.H. Suh, D.G. Churchill, *Chem. Commun.* 2012, **48**, 7298.

Dalton Transactions Accepted Manuscript

40. (a) S.T. Manjare, S. Kim, W.D. Heo, D.G. Churchill, *Org.Lett.* 2014, **16**, 410. (b) S.R. Liu, S.P. Wu, *Org. Lett.* 2013, 15, 878. (c) B. Wang, P. Li, F. Yu, P. Song, X. Sun, S. Yang, Z. Lou, K. Han, *Chem. Commun.* 2013, **49**, 1014. (d) Z. Lou, P. Li, Q. Pan, K. Han, *Chem. Commun.* 2013, **49**, 2445. (e) B. Wang, F. Yu, P. Li, X. Sun, K. Han, *Dyes Pigm.* 2013, **96**, 383. (f) C. Sun, W. Shi, Y. Song, W. Chen, H. Ma, *Chem. Commun.* 2011, **47**, 8638.

41. (a) S.T. Manjare, S. Kim, Y. Lee, D.G. Churchil, *Org.Lett.* 2014, **16**, 520. b) A. Kumar, J.D. Singh, *Inorg. Chem.* 2012, **51**, 772. c) J.D. Singh, M. Maheshwari, S. Khan, R.J. Butcher, *Tet.Lett.* 2008, **49**, 117. d) M. Maheshwari, S. Khan, J.D. Singh, *Tet.Lett.* 2007, **48**, 4737.

42. C.W. McDaniel, J.S. Bradshaw, K.H. Tarbet, G.C. Lindh, R.M. Izatt, *J Incl Phenom Macrocycl Chem*, 1989, **7**, 545.

43. (a) R.L. Davidovich, V. Stavila, D.V. Marinina, E.I. Voita, K.H. Whitmire, *Coord. Chem. Rev.* 2009, **253**, 1316. (b) R.L. Davidovich, V. Stavila, K.H. Whitmire, *Coord. Chem. Rev.* 2010, **254**, 2193.

44. P.N. Basa, A.G. Sykes, *J. Org. Chem.* 2012, **77**, 8428.

45. Slow evaporation of **6** in CH_2Cl_2 solution yielded yellow blocks, but the quality of the crystal is very poor and we were able to determine the cell parameters only. Cell parameters for **6**: a = 7.42Å; b = 7.56 Å; c = 11.62 Å; α = 93.14°; β = 97.73°; γ = 105.47°. Volume = 619 $Å^3$ and space group is Triclinic.

46. J.R. Lakowicz, *Principles of Fluorescence Spectroscopy*. Editor, Springer-Scientific, 2006, p. 277.

47. A.W. Adamson, J.N. Demas, *The Journal of Physical Chemistry* 1971, **75**, 2463.

Dalton Transactions Accepted Manuscript

48. (a) Hohenberg, P.; Kohn, W., Inhomogeneous electron gas. *Physical review* **1964,** *136* (3B), B864; (b) Becke, A. D., Density□functional thermochemistry. III. The role of exact exchange. *The Journal of Chemical Physics* **1993,** *98* (7), 5648-5652; (c) Stephens, P.; Devlin, F.; Chabalowski, C.; Frisch, M. J., Ab initio calculation of vibrational absorption and circular dichroism spectra using density functional force fields. *The Journal of Physical Chemistry* **1994,** *98* (45), 11623-11627; (d) Dunning, T. H., Jr.; Hay, P. J., Gaussian Basis Sets for Molecular Calculations. In *Methods of Electronic Structure Theory*, Schaefer, H., III, Ed. Springer US: 1977; Vol. 3, pp 1-27; (e) Hay, P. J.; Wadt, W. R., Ab initio effective core potentials for molecular calculations. Potentials for the transition metal atoms Sc to Hg. *The Journal of Chemical Physics* **1985,** *82* (1), 270-283; (f) Miertuš, S.; Scrocco, E.; Tomasi, J., Electrostatic interaction of a solute with a continuum. A direct utilizaion of AB initio molecular potentials for the prevision of solvent effects. *Chemical Physics* **1981,** *55* (1), 117-129; (g) Bauernschmitt, R.; Ahlrichs, R., Treatment of electronic excitations within the adiabatic approximation of time dependent density functional theory. *Chemical Physics Letters* **1996,** *256* (4), 454-464; (h) Frisch, M. J.; Trucks, G. W.; Schlegel, H. B.; Scuseria, G. E.; Robb, M. A.; Cheeseman, J. R.; Scalmani, G.; Barone, V.; Mennucci, B.; Petersson, G. A.; Nakatsuji, H.; Caricato, M.; Li, X.; Hratchian, H. P.; Izmaylov, A. F.; Bloino, J.; Zheng, G.; Sonnenberg, J. L.; Hada, M.; Ehara, M.; Toyota, K.; Fukuda, R.; Hasegawa, J.; Ishida, M.; Nakajima, T.; Honda, Y.; Kitao, O.; Nakai, H.; Vreven, T.; Montgomery Jr., J. A.; Peralta, J. E.; Ogliaro, F.; Bearpark, M. J.; Heyd, J.; Brothers, E. N.; Kudin, K. N.; Staroverov, V. N.; Kobayashi, R.; Normand, J.; Raghavachari, K.; Rendell, A. P.; Burant, J. C.; Iyengar, S. S.; Tomasi, J.; Cossi, M.; Rega, N.; Millam, N. J.; Klene, M.; Knox, J.

Dalton Transactions Accepted Manuscript

E.; Cross, J. B.; Bakken, V.; Adamo, C.; Jaramillo, J.; Gomperts, R.; Stratmann, R. E.; Yazyev, O.; Austin, A. J.; Cammi, R.; Pomelli, C.; Ochterski, J. W.; Martin, R. L.; Morokuma, K.; Zakrzewski, V. G.; Voth, G. A.; Salvador, P.; Dannenberg, J. J.; Dapprich, S.; Daniels, A. D.; Farkas, Ö.; Foresman, J. B.; Ortiz, J. V.; Cioslowski, J.; Fox, D. J. *Gaussian 09*, Gaussian, Inc.: Wallingford, CT, USA, 2009.

49. M. Bouroushian, *Electrochemistry of Metal Chalcogenides, Monographs in Electrochemistry, Springer-Verlag Berlin Heidelberg,* 2010, *Chapter 2*, 57-75.

50. WinGX: An Integrated System of Windows Programs for the Solution, Refinement, and Analysis of Single Crystal X-ray Diffraction Data, Ver. 1.70, L.J.*J.* Farrugia, *Appl. Cryst.* 1999, **32**, 837.

51. SHELX97 - Programs for Crystal Structure Analysis (Release 97-2). G.M. Sheldrick, *Institüt für Anorganische Chemie der Universität*, Tammanstrasse 4, D-3400 Göttingen, Germany, 1998.

52. A. Altomare, M.C. Burla, M. Camalli, G. Cascarano, C. Giacovazzo, A. Guagliardi, A.G.G. Moliterni, G. Polidori, R. Spagna, Sir97: A new tool for crystal structure determination and refinement. *J. Appl. Cryst.* 1998, **32**, 115.

53. (a) O.V. Dolomanov, L.J. Bourhis, G.R.J. Howard, J.A.K. Puschmann, *J. Appl. Cryst.* 2009, **42**, 339. (b) G.M. Sheldrick, *Acta Cryst.* 2008**, A64**, 112.

54. V. Balasubramanian, *Synthesis of new nitrogen-containing anthraquinone macrocycles for the luminescence detection of heavy metal ions, M.S. Thesis Dissertation's University of South Dakota*, 2011.

Dalton Transactions Accepted Manuscript